THE JOURNAL OF PHYSICAL CHEMISTRY C
A JOURNAL OF THE AMERICAN CHEMICAL SOCIETY

pubs.acs.org/JPCC

Article

Controlling Rectification in Metal−Molecules−Metal Junctions Based on 11-(Ferrocenyl) Undecanethiol: Effects of the Electronic Coupling Strength

Quyen Van Nguyen*

Cite This: J. Phys. Chem. C 2022, 126, 6405−6412

Read Online

ACCESS | Metrics & More | Article Recommendations | Supporting Information

ABSTRACT: We report an effect of contact materials (Ag, Au, and Pt) on transport properties of molecular junctions (MJs) based on self-assembled monolayers of 11-(Ferrocenyl) undecanethiol ($HSC_{11}Fc$). Particularly, we observed that the Fc unit directly contacting the Ag-coated atomic force microscopy (AFM) tip in symmetrical MJs, $Ag/SC_{11}Fc/Ag$, leads to a large rectification (~150) with a giant electrical current density ($\sim 4 \times 10^4$ A·cm^{-2}) at a relatively small negative voltage, −1.5 V. We also observed that the material of the bottom electrode strongly affects the rectified current density but not the rectification ratio in metal/$SC_{11}Fc$/Ag. Optimizing the material of the bottom electrode, especially the energy offset barrier ε_o, can produce a large rectification (~170) at 1.5 V with a giant electrical current, 2.4×10^5 A·cm^{-2}, in asymmetrical MJs using the Ag-coated AFM tip. A simplified Landauer allows us to approximately quantify the electronic coupling strength in symmetrical MJs, $\Gamma_{Fc\text{-}Ag} \sim 5.2$ meV, that is 50 times greater than $\Gamma_{Ag\text{-}Fc}$. In contrast, the electronic coupling strength at the Fc-Au (or Pt) interface is strong ($\Gamma_{Fc\text{-}Au} \sim 120$ meV), which leads to a small rectification and high conductance. The direction of the small rectification in the strong coupling regime ($\Gamma_{Fc\text{-}Au/Pt}$) can be reversed by controlling the work function of the metal contacts. Overall, our results provide a clear picture of the influence of both the electronic coupling strength and the energy offset barrier on the transport properties and further prove that the conductive-probe atomic force microscopy is a useful, versatile tool for determining structure-transport relationships in molecular junctions.

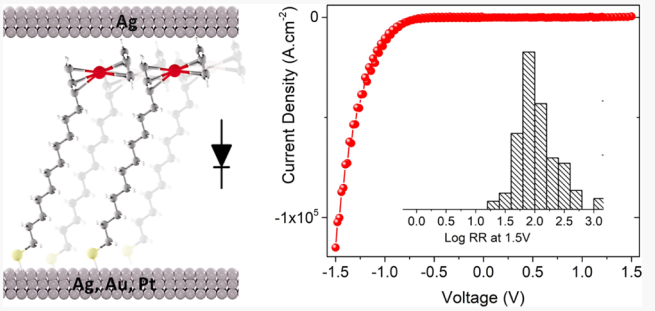

INTRODUCTION

A molecular diode, metal−molecules−metal junctions (MJs), rectifies electrical currents passed through in one bias direction, while it blocks the current in a reversed bias.[1−22] The performance of a molecular diode is usually defined by three main parameters including (i) first, the rectification ratio (RR) defined by using eq 1, (ii) second, the negative voltage (−V) at which the RR is taken, and lastly, (iii) the electrical current or the current density passed through MJs at the studied voltage. If RR is larger than 1, the molecular diode rectifies the electrical current at a negative bias (−V), whereas it rectifies at the reversed bias (+V) when the RR is smaller than 1.

$$RR = \left| \frac{I(-V)}{I(+V)} \right| \quad (1)$$

In 1974, Ratner and Aviram theoretically proposed that a molecule in the form of donor−bridge−acceptor could rectify electrical currents.[1] Since then, two major approaches have been applied to look for a practical solid-state molecular diode. The first one is to design new molecules, for example, single-component molecules containing a donor[9,22] or an acceptor group[8,23−26] asymmetrically positioned inside the junctions, donor−acceptor,[17] and push−pull molecules.[27,28] The second one is to enhance the understanding of the molecule−metal, or conducting electrode, interaction at both interfaces.[19,29−32] To date, the molecular diode has been one of the main objectives in the field of molecular electronics since it is especially useful in understanding charge transport through molecular junctions.

In general, both the chemical structure of a molecule and the electrode−molecule interface at both sides of MJs affect the electronic structure of MJs and eventually the performance of the molecular diode. One would expect that by optimizing both these effects, we could eventually archive the ideal molecular diode which must possess the giant RR (10^3 to 10^6) at relatively small V (e.g., 1) with a giant electrical current passed through. However, reported molecular diodes had (apart from a few exceptions with large values of RR[15,16,19,22,26]) disappointingly small values of RR < 10 for unclear reasons. Therefore, it is

Received: December 23, 2021
Revised: March 22, 2022
Published: April 5, 2022

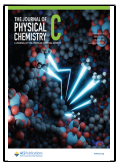

https://doi.org/10.1021/acs.jpcc.1c10806
J. Phys. Chem. C 2022, 126, 6405−6412

important to identify and quantify transport parameters that impact the performance of molecular diodes. Such studies, however, are challenging because (i) molecular junctions are complex physicochemical systems containing not only molecules but also the electronic interaction at both electrode−molecule and molecule−electrode interfaces and lastly (ii) to measure the electronic coupling between molecule−electrode quantitatively or qualitatively is challenging, especially for the molecule−electrode interface where the second electrode is needed to complete the MJs.

To overcome these challenges, one common approach is to systematically design new molecular structures and then study the transport using the same junction's configuration.[16,19,22,26] Another approach is to change the material of the electrodes and keep using the same molecules. The latter approach potentially advances our understanding of the transport properties; however, it is less common since it is especially difficult to change the material of the top electrodes without damaging the molecular layer. The latter approach seemly leads to "contradiction" because the same molecular layer can behave differently depending on the material of the electrode. For instance, MJs based on a 9 nm-thick oligo(bisthienylbenzene) layer with Ti(2 nm)/Au(50 nm) as the top electrode showed a large RR (10^3) at 2.7 V.[19] However, the RR was rapidly decreased 600 times to approximately 1.3 when the carbon conducting layer was used as the top electrode.[33] Nijhuis et al. reported a large RR (RR ~ 10^2 at 1.2 V) for self-assembled monolayer (SAM) MJs based on the 11-(Ferrocenyl)undecanethiol ($HSC_{11}Fc$) molecule (shown in Scheme 1) using the EGaIn top contact.[9,10,15,16] However, with the same molecule, Trasobares et al. reported a very small RR (RR ~ 0.2) at 1.2 V in the reversed direction,[18] and others reported RR ~ 1.[34]

Scheme 1. (A) CP-AFM Setup Where the SAM Substrate is Grounded and the Voltage is Applied to the AFM Tip and (B) Typical Simplified Junction Electronic Structure with Metal Contacts and Potential Energy Level of the HSC11Fc Molecule Involved in the Transport Process

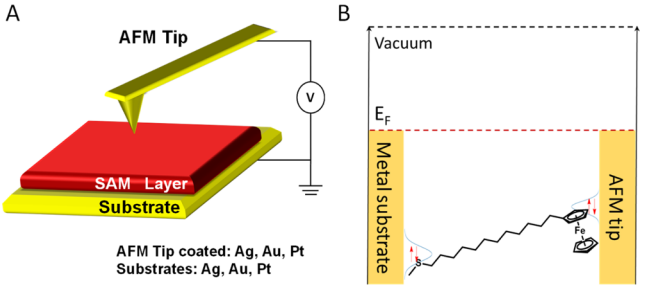

In this study, we aim at understanding the effect of molecule−electrode and electrode−molecule electronic coupling strength on the transport properties and then optimizing the material of the electrode to obtain the best performance of a molecular diode. First, we kept using the $HSC_{11}Fc$ molecule which was widely studied[9,15,16,18] and then investigated the charge transport in SAM MJs by conductive-probe atomic force microscopy (CP-AFM). Second, our CP-AFM setup illustrated in Scheme 1A offers two major advantages: (i) it is an easy, reliable setup to form MJs and study the transport productively; (ii) it allows us to study the effect of electrodes by changing the material of the electrode including Ag, Au, and Pt metals on the transport properties without damaging the SAM molecular layer. Indeed, we observed that the Fc unit qualitatively forms a weak electronic coupling with the Ag metal ($\Gamma_{Fc\text{-}Ag}$ ~ 5.2 meV estimated from the simplified Landauer model), and it results in a large RR, and by optimizing the material of the electrodes, in other words, the electronic coupling at both interfaces, we observed a large rectification of 170 at 1.5 V with giant electrical currents, ~ 2.4×10^5 A·cm^{-2}. If the electronic coupling, in the case of using Au or Pt tips, is strong ($\Gamma_{Fc\text{-}Au}$ ~ 120 meV), the transport properties are different; particularly, a small rectification (~5 at 1.5 V) and high conductance are observed, and interestingly, the direction of the small rectification can be controlled by the work function of the metal contacts.

EXPERIMENTAL METHOD

Materials. Pt and Ti metals were purchased from Kamis, Inc. (Mahopac Falls, NY), and Au nuggets (99.999 purity) and Ag pellets (99.99 purity) were purchased from Mowrey, Inc. (St. Paul, MN) and Kurt J. Lesker Co., respectively. Evaporation boats and Cr evaporation rods were secured from R. D. Mathis (Long Beach, CA). Si(100) wafers were acquired from WaferNet (San Jose, CA). AFM tips (DNP-10 Si_3N_4 contact mode probes) were purchased from Bruker company. 11-(Ferrocenyl) undecanethiol ($HSC_{11}Fc$), 1-decanethiol molecules, and ethyl alcohol (200 Proof) were purchased from Sigma-Alrich company and Supelco, Inc.

Conducting Tip and Sample Preparation. Fabrication of Conducting AFM tips:[21,35−39] Contact mode AFM probes were coated with (i) first an adhesion layer, 5 nm of Cr, and then (ii) 50 nm of Ag or Au metal by using a homemade thermal evaporator. The 5 nm Cr adhesion layer was deposited at a rate of 0.1 to 0.2 nm/s, while 50 nm metallic films were deposited at a rate of 0.5 to 1.0 nm/s. For Pt-coated AFM tips, 5 nm Ti as an adhesion layer and then 20 nm-thick Pt films were e-beam deposited onto the contact mode AFM probe. Afterward, the metal-coated AFM tips were immediately transferred without exposure to air to another glovebox containing the AFM setup for the transport measurements; the area of MJs based on the metal-coated AFM tip was estimated to be approximately 25 nm^2.[36]

Template-stripped flat metal substrates[21,35−39] were employed to grow high-quality SAMs. For flat Ag (or Au) substrates, 500 nm of Ag (or Au) metal was first deposited onto fresh Si(100) wafers by using an e-beam evaporator. For flat Pt substrates, 300 nm of Pt metal was sputter-coated onto a fresh Si wafer at a rate of 0.3 nm/s. On top of the Pt film, subsequent layers of 30 nm of Cr and 200 nm of Au were deposited. The Au film was used to enhance the yield of flat Pt substrates. Si chips (~1 cm^2) were then glued onto the metal surface using epoxy (EPOTEK 377, Epoxy Technologies, MA). The wafer then was cured in an oven at 120 °C for 1 h.

To create SAMs, the ultra-smooth substrates peeled off were immersed in an ethanol solution of 3 mM 11-(Ferrocenyl) undecanethiol in the absence of light and oxygen. After 3 h, the SAM samples were rinsed with the ethanol solvent, then dried in a stream of N_2 gas, and immediately transferred to the AFM glovebox for the transport measurement.[16,22]

X-ray Photoemission and Ultraviolet Photoemission Spectroscopy. The chemical composition of the SAMs on different metals was characterized by X-ray photoemission spectroscopy (XPS) (details in section S1 in the Supporting Information). The XPS measurements were performed by using a PHI Versa Probe III XPS system (ULVAC-PHI) using a monochromatized Al−K X-ray source (1486.6 eV). The base

https://doi.org/10.1021/acs.jpcc.1c10806
J. Phys. Chem. C 2022, 126, 6405−6412

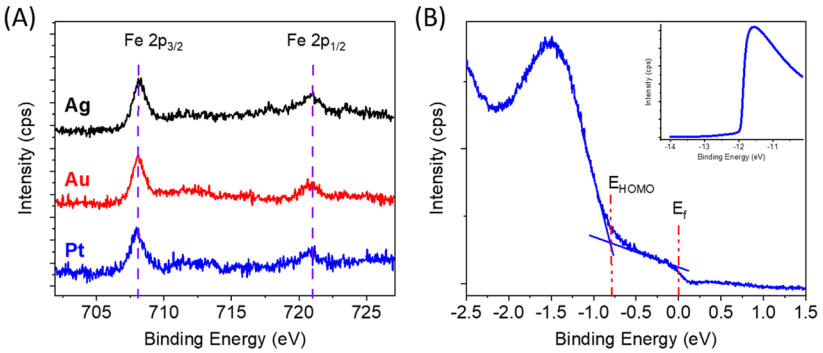

Figure 1. (A) Fe_{2p} High-resolution spectra of the $HSC_{11}Fc$ SAMs on metal substrates. (B) UPS spectra of the SAMs on the Pt substrate show the threshold binding energy (E_{HOMO}) at 0.75 eV with respect to the Fermi level (E_f), and the inset shows the secondary cutoff energy with 5 V applied.

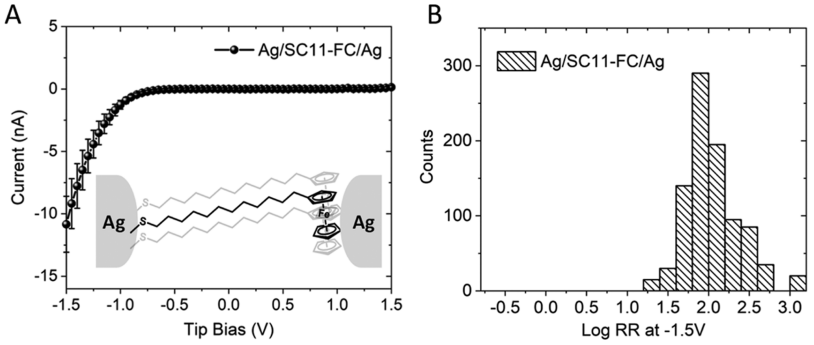

Figure 2. (A) Current−voltage characteristic of Ag-$HSC_{11}Fc$-Ag MJs with standard deviation and (B) corresponding histogram of the RR taken at −1.5 V.

pressure was 5.0×10^{-8} Pa. During XPS measurement, the pressure was approximately 1.0×10^{-6} Pa. The samples were mounted on an XPS sample holder by using a double-sided carbon adhesive tape and then grounded by using a metal spring clip on the holder. The X-ray spot size (diameter) was 100 μm, and the source power was 25 W at 15 kV. The high-resolution C_{1s}, S_{2p}, $Au_{4f,}$ and Fe_{2p} spectra were then collected over several positions. The binding energy scales were referenced to the Au_{4f} peak (84.0 eV). The highest occupied molecular orbital (HOMO)−Fermi level offset of the SAMs on metals was measured by ultraviolet photoemission spectroscopy (UPS) in the same instrument (section S2 in the Supporting Information).

Transport Measurements. CP-AFM-based molecular junctions were fabricated by using an AFM setup (Multimode 8, Bruker). All transport measurements were carried out in an Ar-filled glovebox (MBraun) at ambient temperature. At first, the metal-coated AFM tips were brought into "soft" contact with the SAM layer by applying 1 nN force onto the AFM tip (details in section S3, Supporting Information). Then, the SAM samples were grounded, while voltages (V) were applied to the tip by using a Keithley model 236 electrometer operated in the sweep mode. Voltage was swept in ±1.5 V for the junctions. During the transport measurement, the metal-coated AFM tips are usually tested on the SAM samples of the 1-decanethiol molecule.

RESULTS AND DISCUSSION

We prepared a SAM of the $HSC_{11}Fc$ molecule on various metallic substrates (Ag, Au, and Pt) following the procedure reported previously. To avoid the oxidation of the Ag substrate, The SAM solution was performed in a glovebox filled with N_2 (oxygen level below 0.1 ppm).[16,22] The SAM layers were then characterized by XPS and UPS (details in Sections S1 and S2 in the Supporting Information). The Fe 2p high-resolution spectra of the SAMs on various metals are presented in Figure 1A. The spectra show prominent features at 707.8 and 721 eV, which are associated with the Fe $2p_{3/2}$ and Fe $2p_{1/2}$ doublet, respectively. The spin−orbit splitting is approximately 13.2 eV which is consistent with the previous reports.[16,22]

Figure 1B presents the UPS spectra around the Fermi edge of the Pt/$SC_{11}Fc$ sample and the secondary electron cutoff (an inset). UPS spectra of SAMs on Ag and Au substrates are shown in Figure S2 and Table S1 in the Supporting Information. As seen in Figure 1B, there is a feature peaked at −1.5 eV which can be assigned to the property of the ferrocene unit. The energy offset between the HOMO level and the Fermi level was estimated at −0.75 eV by using the established standard protocol as indicated in Figure 1B.[37,39,40] The energy offset decreased from −0.75 eV (for Pt) to −0.85 eV (for Au) and −1.04 eV for Ag as expected, while all the modified electrodes had a similar work function as shown in Table S1 caused by the interface dipole.

To investigate the transport properties of MJs based on HSC11Fc, we employed the CP-AFM platform, as illustrated in Scheme 1A (details in section S3 in the Supporting Information). Briefly, $HSC_{11}Fc$ molecules formed the SAM layer on an ultrasmooth metallic substrate, named the bottom electrode, and then, the metal-coated probe tip, named the top electrode, was brought into "soft" contact (1 nN) with the SAM layer forming a complete metal−molecule−metal junction. Our junction designations include the molecule used to form the SAM layer and the material of electrode contacts. For example, Au-$HSC_{11}Fc$−Ag MJs indicate the SAM layer made of $HSC_{11}Fc$ molecules, while Au and Ag metals were the bottom and top

https://doi.org/10.1021/acs.jpcc.1c10806
J. Phys. Chem. C 2022, 126, 6405−6412

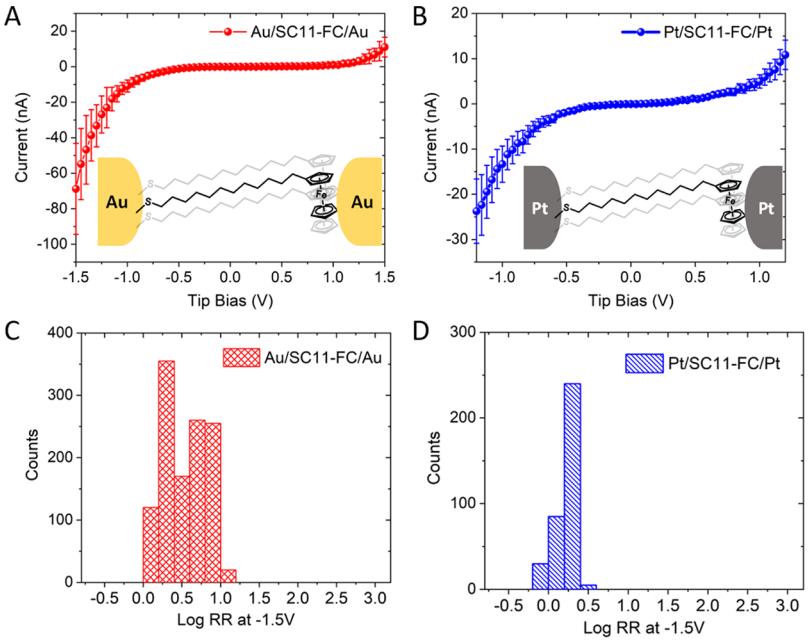

Figure 3. (A) Current−voltage Characteristic of (A) Au-SC11Fc-Au MJs and (B) Pt-SC11Fc-Pt MJs with standard deviation. The histogram of the RR of (C) Au-SC11Fc-Au MJs and (D) Pt-SC11Fc-Pt MJs taken at −1.5 V.

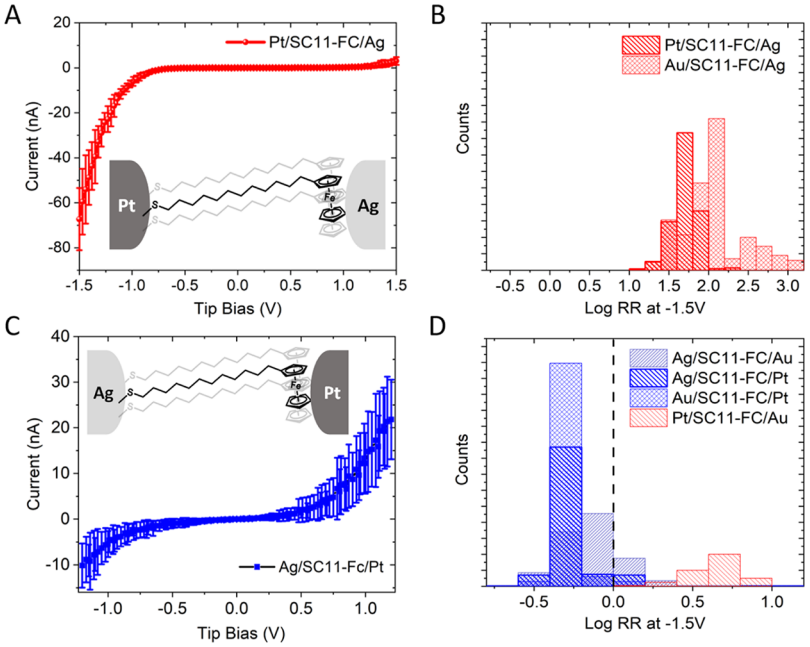

Figure 4. (A) Current−voltage characteristic of Pt-SC11Fc-Ag MJs with standard deviation and (B) corresponding histogram of the RR for the MJs that used Ag as the AFM conductive tip taken at −1.5 V. (C) Current−voltage characteristic of Ag-SC11Fc-Pt MJs with standard deviation and (D) corresponding histogram of the RR.

electrode, respectively. Voltage was then swept at the tip, while the substrate was grounded, the current−voltage (IV) characteristics were then acquired, and 500−1000 *I*−*V* traces were recorded for each sample at several locations. We note that the metal−molecule interface (or the bottom interface) in our MJs is assigned to the metal−S bonding, whereas the molecule−metal interface (or the top interface) means the interaction between the Fc unit and CP-AFM tip.

Figure 2A presents the resulting electrical current−voltage (IV) characteristics of symmetrical Ag-SC_{11}Fc−Ag MJs. As shown, Ag-SC_{11}Fc−Ag MJs did not conduct at a low bias, the electrical current at voltage close to 0 V was out of our limitation detection (∼10 Gohm), and, however, at a higher potential window, the electrical current was rectified at a negative bias, and the electrical current was ∼10 nA at −1.5 V, corresponding to 4×10^4 A·cm^{-2} (the assumed area of the CP-AFM junction is ∼ approximately 25 nm^2). The histogram of the RR taken at −1.5 V was peaked at 150 as shown in Figure 2B which is relatively large for symmetrical MJs. The large rectification is consistent with the report made by Nijhuis et al.[9,15,16] where the EGaIn liquid conductive contact was used as the top electrode. We notice here that in our MJs, the junction is symmetrical with

https://doi.org/10.1021/acs.jpcc.1c10806
J. Phys. Chem. C 2022, 126, 6405−6412

Ag metals at both the bottom and top electrodes. To our knowledge, it is the first report on the large rectification (~150 with a giant current density, 4×10^4 A·cm^{-2}, at low voltage, −1.5 V) for symmetrical, solid-state, and single-component MJs.

Figure 3A,B presents the current−voltage characteristic of Au-SC_{11}Fc-Au and Pt-SC_{11}Fc-Pt MJs, respectively. The corresponding histogram of the RR taken at −1.5 V is shown in Figure 3C,D. It is interesting that MJs using Au or Pt metal slightly rectify the current at a negative bias (similar rectification direction as MJs with Ag contacts), and the RR is relatively small (peaked at six for Au contacts and two for Pt contacts in the histogram). Importantly, we observed that the conductivity of MJs using Au or Pt metals is higher than that using Ag metal. For example, at negative bias, the current of MJs using Pt metal is slightly higher than using Au and 8 times higher than using Ag metals; however, at positive bias, the difference is up to 100 times. Such big differences in the conductivity and RR could hint at a change in the transport mechanism at first glance.

We next examine the transport properties in asymmetrical MJs formed by altering the material of the AFM tip and substrate. First, we systematically studied the MJs by using the same Ag tip and only varying the material of the substrate; in other words, we kept using the same top interface while modifying the bottom interface. Figure 4A presents the $I-V$ characteristic of Pt-SC_{11}Fc-Ag MJs and the corresponding RR in Figure 4B. At first, we observed that the large rectification was retained for these MJs, and the material of the substrate had little effect on the RR (from 150 for Ag and Au to 170 for the Pt substrate). Interestingly, Pt (or Au)-SC_{11}Fc-Ag MJs electrically conducted better than Ag-SC_{11}Fc-Ag MJs, for example, the current at −1.5 V for Pt-SC_{11}Fc-Ag MJs was 60 nA, corresponding to 2.4×10^5 A·cm^{-2} which is almost six times greater than that for Ag-SC_{11}Fc-Ag MJs. At first, we could first exclude the effect of the substrate work function on transport properties since all the modified electrodes have a similar work function. Van Dyck et al.[41] theoretically predicted that the built-in potential forming inside MJs could induce a rectification which was also observed by Clement et al.;[18] however, the RR in our MJs using the Ag tip was large and almost independent on the bottom contact; as a result, we could also neglect the effect of the built-in potential on the transport properties. Then, it is reasonable to assign the transport behavior to the energy offset estimated by UPS which strongly depends on the metal substrate. It is again proven that the transport mechanism operating in the MJs is dominated by the frontier energy level of the ferrocene unit, not by the interfacial state, metal-S bonding, or the dipole formed at the bottom interface.

To further exploit the role of the electrode, we then performed the transport measurement on asymmetrical MJs where the work function of the AFM tip is greater than that of the substrate, or in other words, $W_f^{AFM-Tip} - W_f^{Substrate} > 0$ (see Figure S3 in the Supporting Information). Figure 4C presents the $I-V$ characteristic of Ag-SC_{11}Fc-Pt MJs, and the corresponding histogram of the RR is shown in Figure 4D. Ag-SC_{11}Fc-Pt (or Au) MJs apparently conducted the current greater than Ag-SC_{11}Fc-Ag MJs. For example, the electrical current passed through Ag-SC_{11}Fc--Pt MJs at 1.2 V was 20 nA which is approximately 100 times higher than that passed through Ag-SC_{11}Fc-Ag MJs. Equally important, these junctions only showed a small RR (RR ~ 0.2 at 1.2 V) as shown in Figure 4D, and the rectification direction is opposite to that of symmetrical MJs using Ag, Au, or Pt metal. We notice that the reversed direction associated with a high conductance and small RR was also observed by Trasobares et al. where $W_f^{AFM-Tip} - W_f^{Substrate} > 0$,[18] which was assigned to the built-in potential formed inside MJs. Figure 4D also presents the RR of asymmetrical MJs where the work function of the AFM tip is now higher than that of the substrate, $W_f^{AFM-Tip} - W_f^{Substrate} < 0$. Generally speaking, these junctions showed a high conductance and small RR, and the current was rectified at positive bias, similar to the symmetrical MJs. The direction of the small RR can be easily reversed by only reversing the material used for the substrate and the AFM tip, which could be assigned to the built-in potential formed in MJs.[18,41] For example, Pt− SC_{11}Fc-Au MJs rectified the current at a negative voltage, whereas Au− SC_{11}Fc-Pt MJs rectified the current at a positive voltage as shown in Figure 4D.

To summarize, we have proven the transport properties of MJs including that rectification and conductance depend strongly on the materials of the metal contact, in other words, the electronic coupling strength at the metal−molecule and molecule−metal interface and the frontier orbital level alignment in MJs. Ferrocene−Ag interaction at the top interface, between the Ag AFM tip and the ferrocene unit, led to an RR (150 at −1.5 V) with huge electrical current density (up to 4×10^4 A·cm^{-2}). Optimizing the material of the bottom electrode resulted in a larger rectification, RR ~ 170 at 1.5 V, with a giant current density (~2.4×10^5 A·cm^{-2}) for Pt− SC_{11}Fc−Ag MJs. However, when the ferrocene was directly in contact with Au or Pt AFM tips, a small RR (~5) and high conductance were observed. The direction of the small RR (<5) can be reversed by changing the work function of the metal contact. The small rectification and the reversed rectification direction in asymmetrical MJs could be expected due to several reasons including the dipole moment, asymmetrical molecule, a different interfacial coupling of molecules at the two end electrodes, the built-in potential formed in MJs, and the work function of the contacts.

The main question is to understand why the transport properties are strongly dependent on the material of the contact and can we approximately quantify the transport parameters in the symmetrical MJs, metal−molecules−metal. First, as depicted in Scheme 1A, there are two possible energy levels that could get involved in the transport process. The first one is located at metal-S bonding at the bottom interface, and another one is positioned at the ferrocene−metal interface, the top interface. We can eliminate the former because of the following reasons. First of all, the estimated energy offset barrier as shown in Figure 1B and S2 (in the Supporting Information) (0.75 eV for the Pt substrate) is approximately 0.25 eV lower than the energy offset barrier generated by metal-S bonding at the bottom interface (1 eV for the Pt substrate);[40] the same data were observed for Ag and Au electrodes.[40] Second, the transport properties strongly depend on the top interface where the ferrocene unit is directly in contact with the AFM tip.

At the bottom interface, we reasonably assume that the Fc unit is decoupled with the bottom metal by the alkyl C_{11} chain; in other words, the electronic coupling between the metal-Fc unit (Γ_{Au-Fc}) is very weak, and in average, its strength can be considered equally as $\Gamma_{Ag(Au)-Fc} \sim 0.1$ meV in alkane monothiol MJs.[21,40] We note here that the actual electronic coupling strength, $\Gamma_{Metal-Fc}$, maybe slightly smaller than 0.1 meV due to the longer length of the HSC_{11}Fc molecule.

When the ferrocene unit is directly in contact with Au or Pt metal at the top interface, we assume the interaction would qualitatively form a strong electronic coupling $\Gamma_{Fc-Au(Pt)}$ at the

https://doi.org/10.1021/acs.jpcc.1c10806
J. Phys. Chem. C 2022, 126, 6405−6412

top interface. The assumption was based on the following evidence: (i) first of all, the high conductance observed in our transport measurement and (ii) the strong electronic interaction between ferrocene and the Pt or Au substrate.[42] Indeed, Aragones et al. reported highly efficient coherent tunneling in single-molecule wires of oligoferrocenes with the 80% of the conductance quantum G_o.[42−45] They assigned the highly efficient coherent tunneling to the direct Fc-electrode strong coupling ($\Gamma_{Fc\text{-}Au} \sim 120$ meV) and a very low barrier for electron tunneling. In this case, the frontier orbital level of the Fc unit strongly hybridizes with the metal contact ($\Gamma_{Fc\text{-}Au} \sim 120$ meV) which enables the delocalized electronic system of the organometallic unit, Fc, to be extended to the metal electrode. We note that the $\Gamma_{Fc\text{-}Au} \sim 120$ meV is 1000 times greater than $\Gamma_{Au\text{-}Fc} \sim 0.1$ meV; then, it is reasonable to assume that the voltage will mostly drop at the bottom interface with the weaker coupling strength, which means that the potential of the bottom electrode can move freely while biasing;[13] as a result, a high conductance and a small RR is expected to be observed in MJs using Au or Pt contacts.

In contrast, the Fc unit would form a weaker electronic coupling with the Ag tip, in comparison with the Fc−Au (Pt) interaction, which was supported by a weak electronic interaction between the ferrocene molecule and Ag substrates.[46,47] The charge transport through MJs can be modeled using a single-level model proposed by Larade and Bratkovsky.[5] This model as shown in the inset of Figure 5 and assumes that

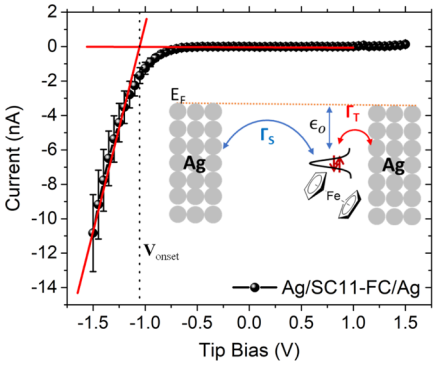

Figure 5. Onset voltage, V_{onset}, was estimated by extrapolating the $I-V$ characteristic of symmetrical Ag/SC_{11}Fc/Ag MJs at a negative voltage regime, corresponding to a weak electronic coupling at the substrate, (Γ_S), and a stronger electronic coupling, Γ_T, at the Ag tip. The inset presented a single-level model assuming that the transport is dominated by a single molecular level of the Fc unit.

the transport is dominated by a single molecular level of the Fc unit. In this case, the Fc unit is coupled to the substrate and the tip through the tunneling rate Γ_S and Γ_T, respectively, which describe the strength of the electronic coupling between the molecules with the substrate and the AFM tip. The ε_o level corresponds to the energy barrier between the highest occupied molecular level or HOMO of the Fc unit and the Fermi level of the Ag contacts.

$$T(E, V) = \frac{4\Gamma_S\Gamma_T}{[E - \varepsilon_o(V)]^2 + \Gamma^2} \quad (2)$$

We next attempt to approximately quantify the electronic coupling strength of the Fc−Ag interaction based on a simple model proposed by Sherif et al.[13] In the spirit of the Landauer formalism, the transport is controlled by the energy- and voltage-dependent transmission $[T(E,V)]$ that is expressed as eq 2. Here, $\Gamma = \Gamma_S + \Gamma_T$ and $\varepsilon_o(V)$ is the level position that is shifted with bias as $\varepsilon_o(V) = \varepsilon_o + (eV/2)[(\Gamma_S - \Gamma_T)/\Gamma]$. This bias dependence takes into account a large portion of the voltage that must drop at the interface with the weaker coupling, the bottom interface in our MJs. When $\Gamma_T > \Gamma_S$, the onset of the current will occur at $eV_{onset} = \varepsilon_0\Gamma/\Gamma_T$, and then, the electronic coupling between the molecule and AFM tip could be quantified if the onset voltage, V_{onset}, is known. We now estimated the onset voltage, $V_{onset} = -1.06$ V, by extrapolating the $I-V$ characteristic of MJs using the Ag tip at a negative voltage regime as shown in Figure 5, and from the onset voltage, we were able to calculate the electronic coupling between the Fc and Ag tip which is approximately $\Gamma_{Fc\text{-}Ag} \sim 5.2$ meV, almost 50 times greater than the electronic coupling between the Ag and Fc unit, $\Gamma_{Ag\text{-}Fc} \sim 0.1$ meV.

By using the simplified model, we were able to approximately quantify the transport parameters in symmetrical MJs based SC_{11}Fc using the Ag conductive AFM tip. We observed that when the electronic coupling strength ($\Gamma_{Fc\text{-}Ag}$) is approximately 5 meV MJs, 50 times greater than $\Gamma_{Ag\text{-}Fc}$, it leads to a large rectification with giant current density, whereas the strong electronic coupling ($\Gamma_{Fc\text{-}Au} \sim 120$ meV), 1000 times greater than that of the bottom interface, and a very low barrier lead to both a small rectification and a change in the transport mechanism.

CONCLUSIONS

In summary, we have demonstrated the effect of the electrode material on the transport properties including rectification and conductance in MJs based on the HSC_{11}Fc molecule. The electronic coupling strength at the Fc-metal interface plays an important role in the transport properties, especially rectification. In particular, the Fc-Ag top interface led to a large rectification (RR ∼ 170) with a giant electrical current density (2×10^5 A·cm^{-2}) at a relatively low voltage, −1.5 V. Using the simplified model based on Landauer theory, we were able to approximately quantify the electronic coupling strength, $\Gamma_{Fc\text{-}Ag} \sim 5.2$ meV, which is almost 50 times larger than $\Gamma_{Fc\text{-}Ag} \sim 0.1$ meV. In this case, the material of the bottom electrode strongly affects the rectified current density which was increased almost 10 times from 4×10^4 A·cm^{-2} for the Ag substrate to 2.4×10^5 A·cm^{-2} for the Pt substrate, while the RR was slightly increased, from 150 for Ag to 170 for Pt. In contrast, the electronic coupling at the Fc-Au (or Pt) interface was strong ($\Gamma_{Fc\text{-}Au} \sim 120$ meV), which led to a small rectification and high conductance, a signature of a change in the transport mechanism. The direction of the small rectification in the strong coupling regime ($\Gamma_{Fc\text{-}Au}$) can be reversed by controlling the work function of the metal contacts.

In addition, we also proved that CP-AFM-based MJs offer several advantages such as simple, fast, and reproducible junction formation; soft contact without damaging the molecular layer; and flexible change of the metal contact that enables rational design approaches to understand the interface effect on the transport properties.

ASSOCIATED CONTENT

Supporting Information

The Supporting Information is available free of charge at https://pubs.acs.org/doi/10.1021/acs.jpcc.1c10806.

XPS and UPS data and transport measurement by CP-AFM (PDF)

https://doi.org/10.1021/acs.jpcc.1c10806
J. Phys. Chem. C 2022, 126, 6405−6412

AUTHOR INFORMATION

Corresponding Author

Quyen Van Nguyen − *Department of Chemical Engineering and Materials Science, University of Minnesota, Minneapolis, Minnesota 55455, United States; Department of Advanced Materials Science and Nanotechnology, University of Science and Technology of Hanoi (USTH), Vietnam Academy of Science and Technology, Hanoi 11307, Vietnam;* orcid.org/0000-0003-0120-0971; Email: nguyen-van.quyen@usth.edu.vn

Complete contact information is available at: https://pubs.acs.org/10.1021/acs.jpcc.1c10806

Notes

The author declares no competing financial interest.

ACKNOWLEDGMENTS

The author thanks Professor C. Daniel Frisbie at the University of Minnesota and Professor Zuoti Xie at the Department of Materials Science and Engineering, Guangdong Technion-Israel Institute of Science, for their invaluable discussion. The author acknowledges the financial support of the National Science Foundation (CHE-2003199) and the Vietnam Academy of Science and Technology (THTEXS.03/21-24). Parts of this work were carried out in the Characterization Facility, the University of Minnesota, which receives partial support from the NSF through the MRSEC (award number DMR-2011401) and NNCI programs (award number ECCS-2025124). Parts of this work were carried out in the Department of Advanced Materials Science and Nanotechnology, University of Science and Technology of Hanoi.

REFERENCES

(1) Aviram, A.; Ratner, M. A. Molecular Rectifiers. *Chem. Phys. Lett.* **1974**, *29*, 277−283.

(2) Vuillaume, D.; Chen, B.; Metzger, R. M. Electron Transfer through a Monolayer of Hexadecylquinolinium Tricyanoquinodimethanide. *Langmuir* **1999**, *15*, 4011−4017.

(3) Chabinyc, M. L.; Chen, X.; Holmlin, R. E.; Jacobs, H.; Skulason, H.; Frisbie, C. D.; Mujica, V.; Ratner, M. A.; Rampi, M. A.; Whitesides, G. M. Molecular Rectification in a Metal−Insulator−Metal Junction Based on Self-Assembled Monolayers. *J. Am. Chem. Soc.* **2002**, *124*, 11730−11736.

(4) Mujica, V.; Ratner, M. A.; Nitzan, A. Molecular rectification: why is it so rare? *Chem. Phys.* **2002**, *281*, 147−150.

(5) Larade, B.; Bratkovsky, A. M. Current rectification by simple molecular quantum dots: Anab initiostudy. *Phys. Rev. B* **2003**, *68*, 235305.

(6) Lenfant, S.; Krzeminski, C.; Delerue, C.; Allan, G.; Vuillaume, D. Molecular Rectifying Diodes from Self-Assembly on Silicon. *Nano Lett.* **2003**, *3*, 741−746.

(7) Elbing, M.; Ochs, R.; Koentopp, M.; Fischer, M.; von Hänisch, C.; Weigend, F.; Evers, F.; Weber, H. B.; Mayor, M. A single-molecule diode. *Proc. Natl. Acad. Sci. U.S.A.* **2005**, *102*, 8815−8820.

(8) Díez-Pérez, I.; Hihath, J.; Lee, Y.; Yu, L.; Adamska, L.; Kozhushner, M. A.; Oleynik, I. I.; Tao, N. Rectification and stability of a single molecular diode with controlled orientation. *Nat. Chem.* **2009**, *1*, 635−641.

(9) Nijhuis, C. A.; Reus, W. F.; Whitesides, G. M. Molecular Rectification in Metal−SAM−Metal Oxide−Metal Junctions. *J. Am. Chem. Soc.* **2009**, *131*, 17814−17827.

(10) Nijhuis, C. A.; Reus, W. F.; Whitesides, G. M. Mechanism of rectification in tunneling junctions based on molecules with asymmetric potential drops. *J. Am. Chem. Soc.* **2010**, *132*, 18386−18401.

(11) Zhao, J.; Yu, C.; Wang, N.; Liu, H. Molecular Rectification Based on Asymmetrical Molecule−Electrode Contact. *J. Phys. Chem. C* **2010**, *114*, 4135−4141.

(12) Kim, T.; Liu, Z.-F.; Lee, C.; Neaton, J. B.; Venkataraman, L. Charge transport and rectification in molecular junctions formed with carbon-based electrodes. *Proc. Natl. Acad. Sci. U.S.A.* **2014**, *111*, 10928−10932.

(13) Sherif, S.; Rubio-Bollinger, G.; Pinilla-Cienfuegos, E.; Coronado, E.; Cuevas, J. C.; Agraït, N. Current rectification in a single molecule diode: the role of electrode coupling. *Nanotechnology* **2015**, *26*, 291001.

(14) Van Dyck, C.; Ratner, M. A. Molecular rectifiers: a new design based on asymmetric anchoring moieties. *Nano Lett.* **2015**, *15*, 1577−1584.

(15) Yuan, L.; Breuer, R.; Jiang, L.; Schmittel, M.; Nijhuis, C. A. A Molecular Diode with a Statistically Robust Rectification Ratio of Three Orders of Magnitude. *Nano Lett.* **2015**, *15*, 5506−5512.

(16) Yuan, L.; Nerngchamnong, N.; Cao, L.; Hamoudi, H.; del Barco, E.; Roemer, M.; Sriramula, R. K.; Thompson, D.; Nijhuis, C. A. Controlling the direction of rectification in a molecular diode. *Nat. Commun.* **2015**, *6*, 6324.

(17) Bayat, A.; Lacroix, J.-C.; McCreery, R. L. Control of Electronic Symmetry and Rectification through Energy Level Variations in Bilayer Molecular Junctions. *J. Am. Chem. Soc.* **2016**, *138*, 12287−12296.

(18) Trasobares, J.; Vuillaume, D.; Théron, D.; Clément, N. A 17 GHz molecular rectifier. *Nat. Commun.* **2016**, *7*, 12850.

(19) Nguyen, Q. V.; Martin, P.; Frath, D.; Della Rocca, M. L.; Lafolet, F.; Barraud, C.; Lafarge, P.; Mukundan, V.; James, D.; McCreery, R. L.; Lacroix, J.-C. Control of Rectification in Molecular Junctions: Contact Effects and Molecular Signature. *J. Am. Chem. Soc.* **2017**, *139*, 11913−11922.

(20) Zhang, G.-P.; Wang, S.; Wei, M.-Z.; Hu, G.-C.; Wang, C.-K. Tuning the Direction of Rectification by Adjusting the Location of the Bipyridyl Group in Alkanethiolate Molecular Diodes. *J. Phys. Chem. C* **2017**, *121*, 7643−7648.

(21) Xie, Z.; Bâldea, I.; Frisbie, C. D. Why one can expect large rectification in molecular junctions based on alkane monothiols and why rectification is so modest. *Chem. Sci.* **2018**, *9*, 4456−4467.

(22) Chen, X.; Roemer, M.; Yuan, L.; Du, W.; Thompson, D.; del Barco, E.; Nijhuis, C. A. Molecular diodes with rectification ratios exceeding 105 driven by electrostatic interactions. *Nat. Nanotechnol.* **2017**, *12*, 797−803.

(23) Hihath, J.; Bruot, C.; Nakamura, H.; Asai, Y.; Díez-Pérez, I.; Lee, Y.; Yu, L.; Tao, N. Inelastic transport and low-bias rectification in a single-molecule diode. *ACS Nano* **2011**, *5*, 8331−8339.

(24) Souto, M.; Yuan, L.; Morales, D. C.; Jiang, L.; Ratera, I.; Nijhuis, C. A.; Veciana, J. Tuning the Rectification Ratio by Changing the Electronic Nature (Open-Shell and Closed-Shell) in Donor-Acceptor Self-Assembled Monolayers. *J. Am. Chem. Soc.* **2017**, *139*, 4262−4265.

(25) Li, X.-M.; Wang, Y.-H.; Seng, J.-W.; Zheng, J.-F.; Cao, R.; Shao, Y.; Chen, J.-Z.; Li, J.-F.; Zhou, X.-S.; Mao, B.-W. z-Piezo Pulse-Modulated STM Break Junction: Toward Single-Molecule Rectifiers with Dissimilar Metal Electrodes. *ACS Appl. Mater. Interfaces* **2021**, *13*, 8656−8663.

(26) Park, J.; Belding, L.; Yuan, L.; Mousavi, M. P. S.; Root, S. E.; Yoon, H. J.; Whitesides, G. M. Rectification in Molecular Tunneling Junctions Based on Alkanethiolates with Bipyridine-Metal Complexes. *J. Am. Chem. Soc.* **2021**, *143*, 2156−2163.

(27) Zhang, G.-P.; Hu, G.-C.; Song, Y.; Li, Z.-L.; Wang, C.-K. Modulation of Rectification in Diblock Co-oligomer Diodes by Adjusting Anchoring Groups for Both Symmetric and Asymmetric Electrodes. *J. Phys. Chem. C* **2012**, *116*, 22009−22014.

(28) Meany, J. E.; Johnson, M. S.; Woski, S. A.; Metzger, R. M. Surprisingly Big Rectification Ratios for a Very Small Unimolecular Rectifier. *ChemPlusChem* **2016**, *81*, 1152−1155.

(29) Zhao, J.-M.; Chen, L.-Y.; Li, Y.-J.; Shi, N.-P.; Sun, Y.-Z.; Huang, H.; Zhang, G.-P. Greatly improving the rectifying performance of single-molecule diodes through molecular structure design and electrode material optimization. *Phys. E* **2021**, *130*, 114691.

(30) Zhang, G.; Ratner, M. A.; Reuter, M. G. Is Molecular Rectification Caused by Asymmetric Electrode Couplings or by a Molecular Bias Drop? *J. Phys. Chem. C* **2015**, *119*, 6254−6260.
(31) Wei, M.-Z.; Yu, X.; Fu, X.-X.; Wang, Z.-Q.; Wang, C.-K.; Zhang, G.-P. Controlling Rectification Performance by Tuning Molecule-Electrode Coupling Strength in Ferrocenyl-Undecanethiolate Molecular Diodes. *J. Phys. Chem. C* **2018**, *123*, 1559−1565.
(32) Capozzi, B.; Xia, J.; Adak, O.; Dell, E. J.; Liu, Z.-F.; Taylor, J. C.; Neaton, J. B.; Campos, L. M.; Venkataraman, L. Single-molecule diodes with high rectification ratios through environmental control. *Nat. Nanotechnol.* **2015**, *10*, 522−527.
(33) Yan, H.; Bergren, A. J.; McCreery, R.; Della Rocca, M. L.; Martin, P.; Lafarge, P.; Lacroix, J. C. Activationless charge transport across 4.5 to 22 nm in molecular electronic junctions. *Proc. Natl. Acad. Sci. U.S.A.* **2013**, *110*, 5326−5330.
(34) Han, B.; Li, Y.; Ji, X.; Song, X.; Ding, S.; Li, B.; Khalid, H.; Zhang, Y.; Xu, X.; Tian, L.; Dong, H.; Yu, X.; Hu, W. Systematic Modulation of Charge Transport in Molecular Devices through Facile Control of Molecule−Electrode Coupling Using a Double Self-Assembled Monolayer Nanowire Junction. *J. Am. Chem. Soc.* **2020**, *142*, 9708−9717.
(35) Xie, Z.; Bâldea, I.; Smith, C. E.; Wu, Y.; Frisbie, C. D. Experimental and Theoretical Analysis of Nanotransport in Oligophenylene Dithiol Junctions as a Function of Molecular Length and Contact Work Function. *ACS Nano* **2015**, *9*, 8022−8036.
(36) Xie, Z.; Bâldea, I.; Demissie, A. T.; Smith, C. E.; Wu, Y.; Haugstad, G.; Frisbie, C. D. Exceptionally Small Statistical Variations in the Transport Properties of Metal-Molecule-Metal Junctions Composed of 80 Oligophenylene Dithiol Molecules. *J. Am. Chem. Soc.* **2017**, *139*, 5696−5699.
(37) Xie, Z.; Bâldea, I.; Frisbie, C. D. Determination of Energy-Level Alignment in Molecular Tunnel Junctions by Transport and Spectroscopy: Self-Consistency for the Case of Oligophenylene Thiols and Dithiols on Ag, Au, and Pt Electrodes. *J. Am. Chem. Soc.* **2019**, *141*, 3670−3681.
(38) Nguyen, Q. V.; Frisbie, C. D. Hopping Conductance in Molecular Wires Exhibits a Large Heavy-Atom Kinetic Isotope Effect. *J. Am. Chem. Soc.* **2021**, *143*, 2638−2643.
(39) Nguyen, Q. V.; Xie, Z.; Frisbie, C. D. Quantifying Molecular Structure-Tunneling Conductance Relationships: Oligophenylene Dimethanethiol vs Oligophenylene Dithiol Molecular Junctions. *J. Phys. Chem. C* **2021**, *125*, 4292−4298.
(40) Xie, Z.; Bâldea, I.; Frisbie, C. D. Energy Level Alignment in Molecular Tunnel Junctions by Transport and Spectroscopy: Self-Consistency for the Case of Alkyl Thiols and Dithiols on Ag, Au, and Pt Electrodes. *J. Am. Chem. Soc.* **2019**, *141*, 18182−18192.
(41) Van Dyck, C.; Bergren, A. J. Large Built-In Fields Control the Electronic Properties of Nanoscale Molecular Devices with Dipolar Structures. *Adv. Electron. Mater.* **2018**, *4*, 1700656.
(42) Aragonès, A. C.; Darwish, N.; Ciampi, S.; Jiang, L.; Roesch, R.; Ruiz, E.; Nijhuis, C. A.; Díez-Pérez, I. Control over Near-Ballistic Electron Transport through Formation of Parallel Pathways in a Single-Molecule Wire. *J. Am. Chem. Soc.* **2019**, *141*, 240−250.
(43) Paul, R.; Reifenberger, R. G.; Fisher, T. S.; Zemlyanov, D. Y. Atomic Layer Deposition of FeO on Pt(111) by Ferrocene Adsorption and Oxidation. *Chem. Mater.* **2015**, *27*, 5915−5924.
(44) Braun, K.-F.; Iancu, V.; Pertaya, N.; Rieder, K.-H.; Hla, S.-W. Decompositional Incommensurate Growth of Ferrocene Molecules on a Au(111) Surface. *Phys. Rev. Lett.* **2006**, *96*, 246102.
(45) Quardokus, R. C.; Wasio, N. A.; Forrest, R. P.; Lent, C. S.; Corcelli, S. A.; Christie, J. A.; Henderson, K. W.; Alex Kandel, S. Adsorption of diferrocenylacetylene on Au(111) studied by scanning tunneling microscopy. *Phys. Chem. Chem. Phys.* **2013**, *15*, 6973−6981.
(46) Woodbridge, C. M.; Pugmire, D. L.; Johnson, R. C.; Boag, N. M.; Langell, M. A. HREELS and XPS Studies of Ferrocene on Ag(100). *J. Phys. Chem. B* **2000**, *104*, 3085−3093.
(47) Waldfried, C.; Welipitiya, D.; Hutchings, C. W.; de Silva, H. S. V.; Gallup, G. A.; Dowben, P. A.; Pai, W. W.; Zhang, J.; Wendelken, J. F.; Boag, N. M. Preferential Bonding Orientations of Ferrocene on Surfaces. *J. Phys. Chem. B* **1997**, *101*, 9782−9789.

https://doi.org/10.1021/acs.jpcc.1c10806
J. Phys. Chem. C 2022, 126, 6405−6412